

## Using kinetic cellular automata for modeling CO oxidation over Pd<sub>110</sub> surface\*

Valentina Markova, Anastasya Sharifulina

**Abstract.** For simulating CO catalytic oxidation on platinum-group metals, kinetic asynchronous cellular automata (CA) (asynchronous CA with probabilistic transition rules) are used being sometimes referred to as Monte Carlo methods. In this paper, the influence of the rate coefficients values of oxygen adsorption and carbon monoxide absorption on the reaction rate on the catalytic surface is experimentally investigated. A range of the main rate coefficients values for which the reaction exists, is defined. Parallel implementation of approximation of kinetic cellular automata with block-synchronous cellular automata are elaborated and investigated.

### 1. Introduction

The CO catalytic oxidation on platinum-group metals [1, 2] is a classical model reaction of heterogeneous catalysis which, in addition to academic interest has an important practical use in connection with an ecological problem of purification of exhausted gases from carbon oxide admixtures. All the processes, taking place on the catalyst surface consist of a variety of elementary interactions of atoms and molecules. All interactions occur asynchronously, and the probability of each interaction is determined by physical parameters. Conventional modeling methods, based on solutions of differential equations, turned out to be inadequate for description and analysis of catalytic oxidation reactions. This is associated with the fact that they do not take into account the diffusion of molecules over the catalyst surface, a possible change in the atomic structure of the surface under the influence of a reaction medium, etc. [1].

A more effective description of the catalytic oxidation mechanism is a class of kinetic cellular automata (asynchronous cellular automata with probabilistic transition rules) introduced in [5]. In other areas of knowledge, the kinetic cellular automata (CA) simulation methods are referred to as Monte Carlo methods. Based on the properties of surface reactions (the number of molecules on the surface and the speed of their movement) kinetic CA should have huge cellular arrays and a long evolution. It is obvious that simulating such processes in the real time mode can only be done with the

---

\*Supported by Presidium of Russian Academy of Sciences, Basic Research Program No. 2 (2009), and Siberian Branch of Russian Academy of Sciences, Interdisciplinary Project No. 32 (2009).

help of a supercomputer. It has been known that asynchronous CA have no efficient and simple parallel implementation. To reduce the modeling time, the idea to introduce a partial synchronization of operation in asynchronous CA were conceived [3–6]. Here, approximation of an asynchronous cellular automaton with a block-synchronous CA [3] is used for parallelization of kinetic CA.

This paper is organized as follows. Apart from Introduction and Conclusion, it contains six sections. The CO catalytic oxidation reaction over Pd<sub>110</sub> surface is discussed in Section 2. In Section 3, a kinetic cellular automaton is defined. Investigation of the CO oxidation reaction is carried out in Section 4. In Section 5, transformation of an asynchronous CA to a block-synchronous CA and comparison of both modes of operation in cellular automata are proposed. Section 6 is dedicated to the parallel implementation of block-synchronous CA.

## 2. CO oxidation reaction over Pd<sub>110</sub> surface

It is known that CO catalytic oxidation on the surface of Pd<sub>110</sub> is described by the following elementary actions [1, 2]:

1.  $O_{2(\text{gas})} + 2\star \xrightarrow{k_1} 2O_{\text{ads}}$ —oxygen adsorption and dissociation;
2.  $CO_{\text{gas}} + \star \xrightleftharpoons[k_{-2}]{k_2} CO_{\text{ads}}$ —adsorption and desorption of carbon monoxide;
3.  $CO_{\text{ads}} + O_{\text{ads}} \longrightarrow CO_{2(\text{gas})} + 2\star$ —reaction between adsorbed carbon monoxide and adsorbed oxygen;
4.  $O_{\text{ads}} + \star_\nu \xrightarrow{k_4} [\star O_{\text{sub}}]$ —formation of the subsurface oxygen;
5.  $CO_{\text{ads}} + [\star O_{\text{sub}}] \xrightarrow{k_5} CO_{2(\text{gas})} + 2\star + \star_\nu$ —reaction between adsorbed carbon monoxide and subsurface oxygen;
6.  $CO_{\text{gas}} + [\star O_{\text{sub}}] \xrightleftharpoons[k_{-6}]{k_6} [CO_{\text{ads}} * O_{\text{sub}}]$ —formation of the complex;
7.  $[CO_{\text{ads}} * O_{\text{sub}}] \xrightarrow{k_7} CO_{2(\text{gas})} + 2\star + \star_\nu$ —decomposition of the complex;
8.  $CO_{\text{ads}} + \star \xrightarrow{k_8} \star + CO_{\text{ads}}$ —diffusion along the surface;
9.  $CO_{\text{ads}} + [\star O_{\text{sub}}] \xrightarrow{k_8} \star + [CO_{\text{ads}} * O_{\text{sub}}]$ —formation of the complex;
10.  $[CO_{\text{ads}} * O_{\text{sub}}] + [\star O_{\text{sub}}] \xrightarrow{k_8} [\star O_{\text{sub}}] + [CO_{\text{ads}} * O_{\text{sub}}]$ —diffusion of the complex.

Here the symbols  $\star$  and  $\star_\nu$  are the active sites on the surface and the subsurface layers, respectively,  $k_i$ ,  $i = 1, 2, 4, 5, 6, 7$ , and  $k_{-i}$ ,  $i = 2, 6$ , are the rate coefficients for the direct and the reverse  $i$ th action of the reaction;  $k_8$  is the rate of reagents motion along the surface, it is defined by

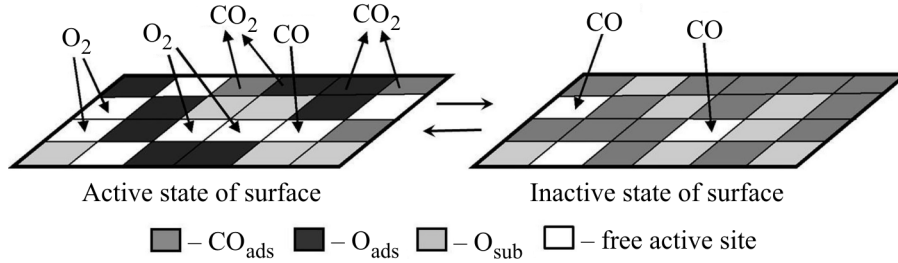


**Figure 1.** Periodical transition of the surface from active to inactive state

$M_{\text{dif}} \times \sum_{j=1}^7 k_j$ , where  $M_{\text{dif}}$  is a diffusion parameter. All the steps of oxidation reaction occur asynchronously and are carried out with a certain probability  $p_i = k_i / \sum_{j=1}^8 k_j$ .

CO oxidation on platinum group metals is accompanied by oscillations of the reaction rate and adsorbed species concentrations. The driving force of the oscillations is associated with a relatively slow formation and consumption of the subsurface oxygen with periodical transitions of metal from an inactive to a highly active catalytic state. This transition occurs as follows. At the initial time, the catalyst surface is free, it corresponds to its active state (Figure 1). Carbon monoxide and oxygen are adsorbed on the catalyst surface from the gaseous phase. Then  $\text{CO}_{\text{ads}}$  molecules and atoms of  $\text{O}_{\text{ads}}$  enter into the reaction with  $\text{CO}_2$  molecules formation.  $\text{CO}_2$  desorbs, and two neighboring sites become free. Simultaneously, atomic oxygen  $\text{O}_{\text{ads}}$  is transformed into the subsurface oxygen. This is accompanied by a decrease in the value of the sticking coefficient of oxygen. As a result, adsorption of oxygen is blocked, and molecules of  $\text{CO}_{\text{ads}}$  are accumulated on the surface, and the amount of the formed  $\text{CO}_2$  is decreased. This corresponds to an inactive state of the surface. The obtained molecules of  $\text{CO}_{\text{ads}}$  diffuse over the surface to the sites occupied by  $\text{O}_{\text{sub}}$ .  $\text{CO}_{\text{ads}}$  and  $\text{O}_{\text{sub}}$  enter into the reaction with formation of free sites for the oxygen and carbon monoxide adsorption. Thereafter the surface again becomes active.

### 3. Kinetic cellular automata for modeling the CO oxidation reaction

A kinetic CA is defined by a multitude  $\mathcal{N}_a = \langle A, M, T, \Theta \rangle$ , where  $A$  is a state alphabet,  $M$  is a naming set,  $T$  is a set of used templates,  $\Theta$  is a set of substitutes performing the oxidation reaction stages,  $a$  is an asynchronous function mode.

The state alphabet of a cell is the set  $A = \{*, \text{CO}_{\text{ads}}, \text{O}_{\text{ads}}, \text{O}_{\text{sub}}, [\text{CO}_{\text{ads}} * \text{O}_{\text{sub}}]\}$ , whose symbols denote the active surface centers, atoms and molecules taking part in the oxidation reaction. The naming set  $M = \{(i, j) : i = 0, 1, \dots, I, j = 0, 1, \dots, J\}$  represents the catalyst surface.

A pair  $(a, (i, j)) \in A \times M$  is called a *cell* (a site on the catalyst surface). Each cell corresponds to a finite-state automaton with the name  $(i, j)$  and the state  $a$ . A set of cells  $\Omega = \{(a, (i, j)) : (i, j) \in A, a = a(i, j) \in M\}$  forms a *cellular array* ( $\Omega(0)$  is the initial state of the cellular array).

On the set  $M$ , a naming function  $\varphi : M \rightarrow M$  is defined. A set of naming functions for a cell with the name  $(i, j) \in M$  determines a *template*

$$T(i, j) = \{(i, j), \varphi_1(i, j), \dots, \varphi_q(i, j)\}. \quad (1)$$

Template (1) enumerates the names of neighbors of a given central cell with the name  $(i, j) \in M$  (*neighborhood*). The commonly encountered template is a “cross”:  $T(i, j) = \{(i, j), (i-1, j), (i, j+1), (i+1, j), (i, j-1)\}$ . A set of cells with the names from template (1),

$$S(i, j) = \{(v_0, (i, j)), (v_1, \varphi_1(i, j)), \dots, (v_q, \varphi_q(i, j))\},$$

is called a *local configuration*,  $T(i, j)$  being its *underlying template*. The cell  $(v_0, (i, j))$  is further referred to as a *reference cell* for the configuration  $S(i, j)$ . The two local configurations  $S(i, j)$  and  $S'(i, j)$  with the same reference cell, whose underlying templates are written in the form of *substitution*

$$\Theta(i, j) : S(i, j) \xrightarrow{p} S'(i, j), \quad (2)$$

where  $S'(i, j) = \{(u_0, (i, j)), (u_1, \psi_1(i, j)), \dots, (u_r, \psi_r(i, j))\}$ , represent an elementary act of the cellular array updating with probability  $p$ . In our applications, we use substitutions for the left-hand and the right-hand sides, for which the condition  $T(i, j) = T'(i, j)$  holds.

Substitution (2) is applicable to a cell with the name  $(i, j) \in M$  (a cell is randomly chosen) with probability  $p$  if  $S(i, j) \in \Omega(t)$ , where  $\Omega(t)$  is the *global state* of cellular array  $\Omega$  at step  $t$ . Otherwise, nothing happens and an attempt to apply this substitution fails. Application of the substitution  $\Theta(i, j)$  to a cell with the name  $(i, j) \in M$  is as follows.

- The values  $u_k = f_k(v_0, v_1, \dots, v_q)$ ,  $k = 0, 1, \dots, q$ , are calculated.
- The cells states  $(u_k, \varphi_k(i, j))$  are replaced by the obtained values.

Application of the substitution  $\Theta(i, j)$  to any cell is performed in a certain period of discrete time called a *step*. Application of  $\Theta(i, j)$  to all cells of the array transfers its global state  $\Omega(t)$  to the next global state  $\Omega(t+1)$  and is called an *iteration*. According to the mechanism of CO oxidation reaction, the iteration consists of  $|M| \times M_{\text{dif}}$  steps, where  $|M|$  is cell array numbers,  $M_{\text{dif}}$  is a diffusion intensity parameter.

The sequence  $\Omega(0), \Omega(1), \dots, \Omega(t), \dots$  obtained as a result of iterative functioning of kinetic CA is called an *evolution*. The evolution describes the dynamics of a catalytic oxidation reaction on a microscopic level.

As an example, let us consider a substitution, which simulates Step 1 of the reaction. Here  $A = \{*, O_{\text{ads}}\}$ . A molecule of oxygen is adsorbed from gas to the two neighboring free cells with probability  $p$ . For a cell named  $(i, j)$ , a name of one of its neighbors is determined by the function:

$$\varphi(i, j) = \begin{cases} (i-1, j), & 0 \leq r \leq 0.25, \\ (i, j-1), & 0.25 < r \leq 0.5, \\ (i+1, j), & 0.5 < r \leq 0.75, \\ (i, j+1), & 0.75 < r \leq 1, \end{cases}$$

where  $r$  is a random number. As a result, the oxygen adsorption reaction is described by the following substitution:

$$\Theta(i, j) : \{(*, (i, j)), (*, \varphi(i, j))\} \xrightarrow{p} \{(O_{\text{ads}}, (i, j)), (O_{\text{ads}}, \varphi(i, j))\}.$$

#### 4. Investigation of the CO oxidation reaction

**4.1. Studying the CO oxidation reaction dynamics.** In the experiments conducted, the oxidation reaction dynamics is represented by the evolution of kinetic CA of size  $400 \times 400$ . The boundary conditions are periodical. In the initial conditions, all cells are active. The oscillatory behavior was observed with the following rate coefficients for the reaction steps

$$\begin{array}{cccc} k_1 = 1, & k_2 = 1, & k_{-2} = 0.2, & k_4 = 0.03, \\ k_5 = 0.01, & k_6 = 1, & k_{-6} = 0.5, & k_7 = 0.02 \end{array}$$

and  $M_{\text{dif}} = 50$ . This set of values was obtained in [2] as a result of calculation experiments.

The CO oxidation reaction dynamics is presented Figure 2. This figure shows the oscillations of values of the reagent concentration ( $O_{\text{ads}}$ ,  $O_{\text{sub}}$ ,  $\text{CO}_{\text{ads}}$ ) and the reaction rate. The reagent concentration on the surface is determined by a share of cells being in a state corresponding to this reagent in a cellular array. The reaction rate is defined by the amount of molecules  $\text{CO}_2$  formed in one cell per iteration.

It has been found experimentally that an amplitude and oscillations of a concentration period for each reagent and the reaction rate remain constant. Let us consider the behavior of the reaction within the period  $t_1-t_4$ .

Beginning with the moment of the time  $t_1$ , the concentration of  $\text{CO}_{\text{ads}}$  starts to decrease and the concentration of  $O_{\text{ads}}$  sharply rises. Changes in the coverages  $\text{CO}_{\text{ads}} \rightarrow O_{\text{ads}}$  occur via the formation of a wave, whose front is characterized by a high concentration of catalytically active sites responsible for a maximal rate of  $\text{CO}_2$  (Figure 2a).

The obtained  $O_{\text{ads}}$  and  $\text{CO}_{\text{ads}}$  react to form  $\text{CO}_2$  (Figure 2b). At the same time, the concentration of adsorbed oxygen redistributes  $O_{\text{ads}} \rightarrow O_{\text{sub}}$ .

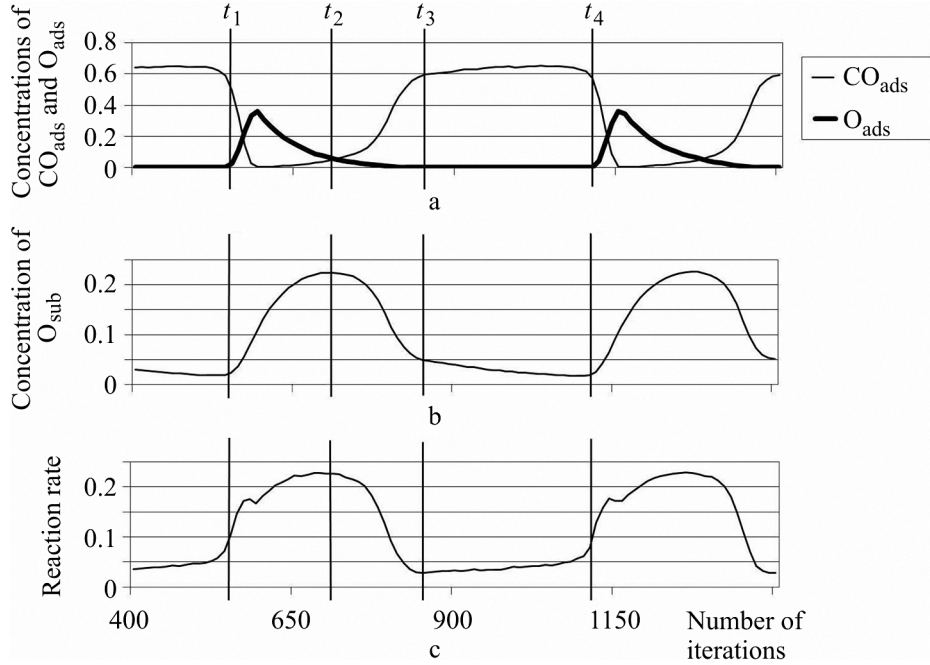


**Figure 2.** The oscillations of concentrations of reagents in the oxidation reaction: a)  $\text{O}_{\text{sub}}$  and  $\text{CO}_{\text{ads}}$ , b)  $\text{O}_{\text{ads}}$ , and c) the reaction rate

The position of a maximum on the curve of the concentration  $\text{O}_{\text{sub}}$ , which is achieved at the time  $t_2$  (Figure 2c), determines the moment of a decrease in the reaction rate. Simultaneously, the catalyst surface accumulates  $\text{CO}_{\text{ads}}$ , this process being accompanied by the complete removal of  $\text{O}_{\text{ads}}$ . A minimal value of the reaction rate is stipulated by the interaction of  $\text{CO}_{\text{ads}}$  only with subsurface oxygen.

At the time  $t_3$ ,  $\text{CO}_{\text{ads}}$  concentration reaches its maximum value. It is conserved for the period  $t_3-t_4$ . A decrease in the  $\text{O}_{\text{sub}}$  concentration towards a critical value (the time  $t_4$ ) again creates favorable conditions for the reaction, and this completes the oscillation cycle. The results of the numerical experiments correspond to the results obtained in [2].

**4.2. A bifurcation diagram of the CO oxidation reaction.** Figure 3 shows a bifurcation diagram of the oxidation reaction in  $(k_1, k_2)$ -parameter space, where the coefficients  $k_1$  and  $k_2$  are the rate coefficients of  $\text{O}_2$  adsorption and CO adsorption, respectively. The diagram was obtained as a result of studying the evolution of a kinetic cellular automaton of size  $400 \times 400$ . In the initial conditions all cells are free. The boundary conditions are periodic. In our calculation experiments, the oscillatory behavior of the reaction rate and reagents concentration was investigated for the following reaction

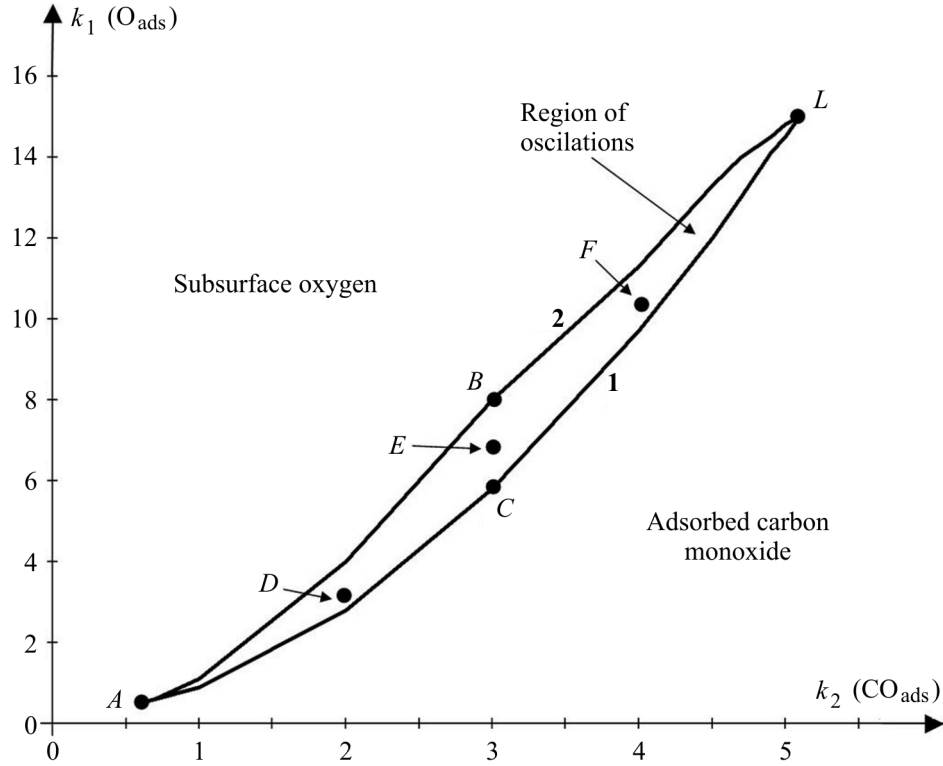


**Figure 3.** A bifurcation diagram of CO oxidation reaction:  $A$  is the point where oscillations begin, Curve 1 is the upper boundary of the region, Curve 2 is the lower boundary of the region,  $L$  is the point where oscillations end

parameters:  $0.5 < k_1 < 20$ ,  $0.6 < k_2 < 6$ ,  $k_{-2} = 0.2$ ,  $k_4 = 0.03$ ,  $k_5 = 0.01$ ,  $k_6 = 1$ ,  $k_{-6} = 0.5$ ,  $k_7 = 0.02$ ,  $M_{\text{dif}} = 50$ .

The experiments have shown that oscillations on a catalyst surface occur in a narrow range of the rate coefficients values  $k_1$  and  $k_2$ . In the figure in question, the oscillations region is limited by the two curves 1 and 2. The region of oscillations begins with the point  $A = (0.6, 0.5)$ , and ends with the point  $L = (15, 5.1)$ . Outside of this range, there are a formation of covering of subsurface oxygen (above Curve 1) and a covering of adsorbed carbon monoxide (under Curve 2).

To study the oxidation reaction dynamics in the oscillations region, let us consider its behavior at several points of the region obtained: at two boundary points  $B$  and  $C$  (Figure 4) and at three inner points  $D$ ,  $E$ , and  $F$  (Figure 5).

As one can see from Figure 4, on the boundaries of this oscillations region, changes in the coverings  $CO_{\text{ads}} \rightarrow O_{\text{sub}}$  on the surface occur very fast and seldom. For the rate coefficient values  $k_1 = 8$  and  $k_2 = 3$ , corresponding

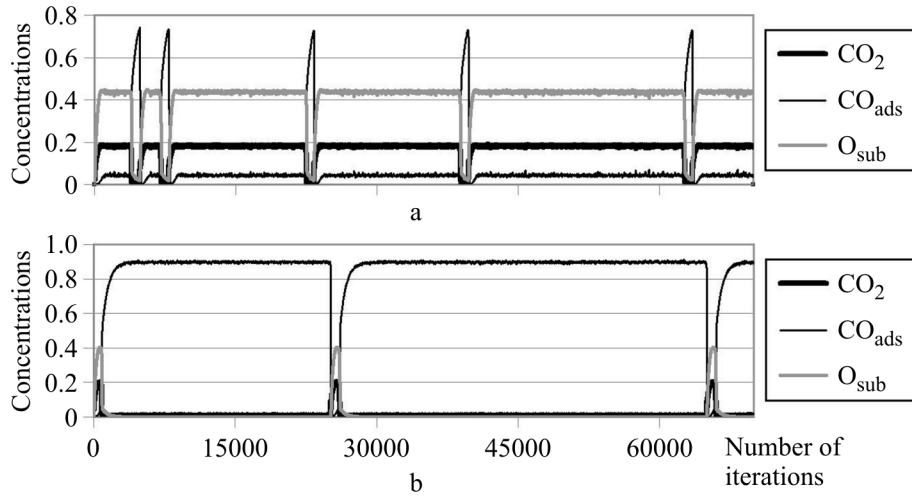


**Figure 4.** Oscillations of the reaction rate and the reagents concentration on the boundaries: a) at the point  $B = (8, 3)$  and b) at the point  $C = (5.8, 3)$

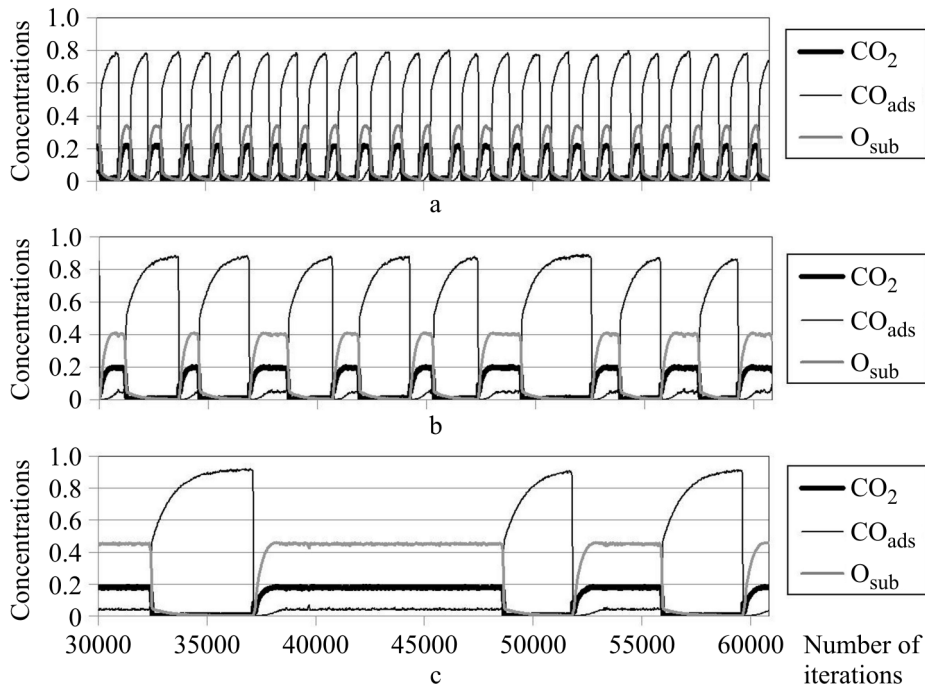


**Figure 5.** Oscillations of the reaction rate and the reagents concentration inside the oscillations region: a) at the point  $D = (3, 2)$ , b) at the point  $E = (7, 3)$ , and c) at the point  $F = (10, 4)$

to the point  $B$  on the upper boundary of region, the catalyst surface is mainly filled with the subsurface oxygen (Figure 4a). Its concentration is significantly higher than the adsorbed carbon monoxide concentration. After 150 iterations, the reaction rate attains the value 0.2, and remains the same over a long period (20,000 iterations). For the rate coefficient values  $k_1 = 5.8$  and  $k_2 = 3$ , corresponding to the point  $C$  on the lower boundary of this region, the catalyst surface is in an inactive state (Figure 4b), really,  $\text{CO}_{\text{ads}}$  concentration comprises 0.9, the subsurface oxygen being essentially lacking. Contrary to the upper boundary of this oscillations region, here a change in the covering of the reaction occurs more rarely (40,000 iterations), on the surface, the oscillations of the rate and of subsurface oxygen occur in the form of delta wave. The rate oscillations amplitude equals 0.2.

Figure 5 demonstrates oscillations of the reaction rate and all reagents concentration on the surface for the rate coefficient values  $k_2$  and  $k_1$  placed inside the oscillations region. The experiments have shown that oscillations have an irregular behavior, the oscillations amplitudes and the period being constant for all listed pointers.

In addition, our experiments have demonstrated that increasing the values of the rate coefficients  $k_2$  and  $k_1$  leads to the following:

1. The period of oscillations of the adsorbed carbon monoxide, the subsurface oxygen, and the reaction rate concentration increases.
2. The amplitudes of the adsorbed carbon monoxide and of the subsurface oxygen oscillations increases.
3. The amplitude of oscillations of the reaction rate does not practically change and is approximately 0.2 for all values of  $k_1$  and  $k_2$  in the region of oscillations.

## 5. Block-synchronous cellular automata for modeling the CO oxidation reaction

In asynchronous CA, each next global state is a result of application of substitutions to all the cells in an array, each being randomly chosen as opposed to synchronous CA. The desire to reduce the simulation time brought about the introduction of partial synchronization of operations in asynchronous CA [3–6]. Here, approximation of an asynchronous CA by a block-synchronous CA is used [5].

**5.1. Algorithm for transformation of asynchronous CA into block-synchronous CA.** The algorithm for transformation of an asynchronous cellular automaton into a block-synchronous one is as follows.

1. On the naming set  $M$ , a *block template*  $T_{B(i,j)} = \{(i,j), \varphi_1(i,j), \dots, \varphi_r(i,j)\}$  is defined. Here the naming functions  $\varphi_1(i,j), \dots, \varphi_r(i,j)$  enumer-

ate  $r$  neighbors of a reference cell with the name  $(i, j)$  involved in substitutions from  $\Theta$ . Denote the block by  $B_{\varphi_k(i,j)} = B_k$ , where  $\varphi_k(i, j)$  is the name of a reference cell.

The block  $B_k$  is characterized by the following features.

- $T_{\Theta(i,j)} \subseteq T_{B_k}$ , where  $T(i, j)$  is an underlying template of substitution from the set  $\Theta$ .
- On the naming set  $M$ , the block template  $B_k$  defines a set of partitions  $\mathcal{M} = \{\mathcal{M}_1, \mathcal{M}_2, \dots, \mathcal{M}_r\}$ , where  $\mathcal{M}_k = \{B_k^1, B_k^2, \dots, B_k^G\}$ . Each partition consists of  $\frac{|\mathcal{M}|}{r}$  blocks. For the blocks of each  $\mathcal{M}_k$  partition, the following relations should hold:

$$\bigcup_g B_k^g = M, \quad \bigcap_g B_k^g = \emptyset, \quad g = 1, 2, \dots, G.$$

Here, the second condition is the correctness one. It requires that any two substitutions do not change the same cell state at the same time.

2. Each iteration time is divided into  $r$  synchronous stages. At the  $k$ th stage,  $k = 1, 2, \dots, r$ , substitutions are applied synchronously to the  $k$ th reference cells of all blocks belonging to the  $k$ th partition.

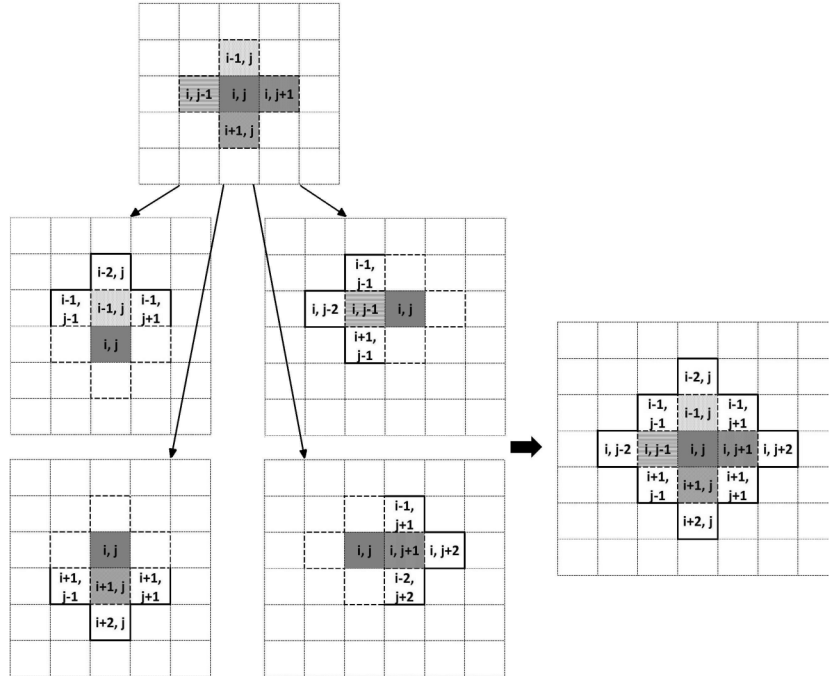
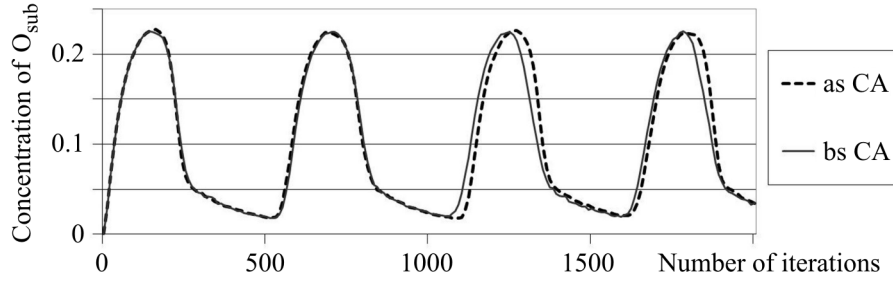


Figure 6. The block template





**Figure 8.** The oscillations of concentrations of  $O_{\text{sub}}$  for asynchronous CA simulating oxidation reaction and its approximation by block-synchronous CA

## 6. Parallel implementation of block-synchronous cellular automata

Parallel implementation of the block-synchronous CA is performed by the domain decomposition method and consists in the following.

1. A cellular array of size  $|M|$  is divided into non-intersecting equal parts, called *domains* (Dom),  $|\text{Dom}| = K \times K = \frac{|M|}{n}$ , where  $n$  is the number of processors used. The domains obtained are allocated to supercomputers processors. The memory of each processor holds its own domain of cells and copies of boundary cells of the neighboring processors. In the initial conditions all domain cells are active.

Figure 9 shows the domains in the  $l$ th and the  $(l+1)$ th processors (here, on the naming set, the partition  $\mathcal{M}_6$  is defined). It is evident that in the course of the decomposition of a cellular array by rectangle domains, certain blocks are shared among the neighboring processors. As a result, a part of substitutions cannot be applied to the reference cell with number 6 if it is

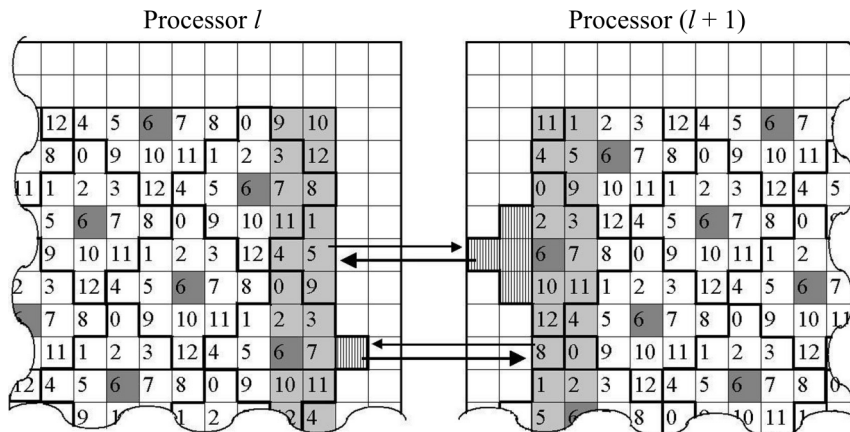


**Figure 9.** Structure of domains in the neighboring processor

a boundary one (Figure 9, the  $l$ th processor) or if it is a near-boundary one (Figure 9, the  $(l + 1)$ th processor). Hence, to apply substitutions to the cell with number 6, the states of the cells with numbers 1, 4, 5, 9 must be sent from the  $l$ th processor to the  $(l + 1)$ th processor and should be written into the corresponding cells to the left of the domain in the first case. And in the second case, the state of the cell with number 8 must be sent from  $(l + 1)$ th processor to the  $l$ th processor and should be written into the corresponding cells to the right of the domain.

2. The evolution iteration of the block-synchronous cellular automaton consists of 13 stages. At each stage, the partition  $\mathcal{M}_l$ ,  $l = 1, \dots, r$ , is randomly chosen. The substitutions of the set  $\Theta$  are synchronously applied to the cells with a chosen number  $l$  in all blocks of the partition  $\mathcal{M}_k$  in all the processors. (The quantity of such cells will be  $\frac{|\text{Dom}|}{r}$ .) After application of substitutions, each processor gives back to the neighboring processors the updated values of their cells. In addition, each processor sends updated values of cells of its own boundary and near-boundary rows (columns) into the neighboring processors. The values of those cells are arranged around the perimeter of the domain. Those four rows (columns) are intended for storage of copies of updated values of the neighboring processors.

The total volume  $V$  of the data exchange, which is sent by each processor to the four neighboring processors, is equal to  $8K$  cells. As a result of the data exchange, each domain has values of all cells which are necessary for execution of the next stage.

The cluster MVS-100K of the Joint Supercomputer Center of the Russian Academy of Sciences was used for parallel implementation of the block-synchronous CA. The basic technical characteristics of MVS-100K are the following: 1460 nodes consisting of two quad-core microprocessors Intel Xeon, the time of transfer of one byte  $t_b = 0.7$  ms, the latency time  $t_{\text{lat}} = 3.2$  ms. The experiments have shown that for the supercomputer MVS-100K the time of application of a substitution to a cell is  $\tau = 0.58$  ms.

According to characteristics of MVS-100K and a well-known condition of efficiency

$$\tau|\text{Dom}| > h(t_{\text{lat}} + Vt_b),$$

where  $h = 13$  is the data exchange number, parallel implementation of the block-synchronous CA will be efficient under the condition

$$|\text{Dom}| > 128 \times 128. \quad (3)$$

The table contains the experimental results of parallel implementation of the block-synchronous CA of sizes  $9000 \times 9000$  and  $12000 \times 12000$  cells. The quality of parallel implementation is estimated by the efficiency of parallelization  $Q(n) = \frac{T_1}{T_n \cdot n}$  and speedup  $S(n) = \frac{T_1}{T_n}$ , where  $T_1$  is computation

Efficiency  $Q(n)$  and speedup  $S(n)$  of parallel implementation

| Parameter                 | $n$     |        |       |       |       |       |
|---------------------------|---------|--------|-------|-------|-------|-------|
|                           | 1       | 4      | 16    | 32    | 64    | 128   |
| Size $9000 \times 9000$   |         |        |       |       |       |       |
| $T_n, s$                  | 568.87  | 146.37 | 37.48 | 18.71 | 9.56  | 4.96  |
| $Q(n)$                    | 1       | 0.97   | 0.95  | 0.95  | 0.93  | 0.89  |
| $S(n)$                    | 1       | 3.9    | 15.2  | 30.4  | 59.5  | 114.7 |
| Size $12000 \times 12000$ |         |        |       |       |       |       |
| $T_n, s$                  | 1005.54 | 256.35 | 66.97 | 33.89 | 16.98 | 8.49  |
| $Q(n)$                    | 1       | 0.98   | 0.94  | 0.93  | 0.93  | 0.92  |
| $S(n)$                    | 1       | 3.9    | 15.0  | 29.7  | 59.2  | 118.4 |

time on one processor,  $T_n$  is computation time on  $n$  processors. The experiments have demonstrated that the parallel implementation of the block-synchronous cellular automaton efficiency is greater than 90 % if condition (3) is met.

## 7. Conclusion

In this paper, the results of investigation of kinetic cellular automaton simulating CO oxidation on surface Pd<sub>110</sub> are presented. The experiments conducted have shown the following:

- The oscillations of the reaction rate occur over surface occur for  $0.5 < k_1 < 14$  and  $0.6 < k_2 < 4.9$ .
- Asynchronous and block-synchronous modes of CA demonstrate the identical behavior. An approximation error is admissible for a probabilistic algorithm.
- Time complexity of block-synchronous CA evolution is less than time complexity of asynchronous CA evolution on a single processor. This fact is associated with a different quantity of generated random numbers.
- Parallel implementation of block-synchronous cellular automaton has the efficiency above 90 %.

## References

- [1] Latkin E.L., Elokhin V.I., Matveev A.V., Gorodetskii V.V. Manifestation of the adsorbed CO diffusion anisotropy caused by the structure properties of the Pd<sub>110</sub>-(1 × 2) surface on the oscillatory behavior during CO oxidation reaction – Monte-Carlo model // Chemistry for Sustainable Development. – 2003. – Vol. 11. – P. 173–180.

- 
- [2] Elokhin V.I., Latkin E.I., Matveev A.V., Gorodetskii V.V. Application of statistical lattice models to the analysis of oscillatory and autowave processes in the reaction of carbon monoxide oxidation over platinum and palladium surfaces // *Kinetics and Catalysis*. — 2003. — Vol. 44, No. 5. — P. 692–700.
  - [3] Toffoli T., Margolus N. *Cellular Automata Machines*. — USA: MIT Press, 1987.
  - [4] Nedeia S.V., Lukkien J.J., Hilbers P.A.J., Jansen A.P.J. Methods for parallel simulations of surface reactions // *Advances in Computation: Theory and Practice, Parallel and Distributed Scientific and Engineering Computing*. — 2004. — Vol. 15. — P. 85–97.
  - [5] Bandman O.L. Synchronous versus asynchronous cellular automata for simulating nano-systems kinetics // *Bull. Novosibirsk Computing Center. Ser. Computer Science*. — Novosibirsk, 1999. — Iss. 25. — P. 1–12.
  - [6] Bandman O.L. Parallel simulation of asynchronous cellular automata evolution // *Proc. ACRI-2006*. — Berlin: Springer, 2007. — P. 41–48. — (LNCS; 4173).

